Progress In Electromagnetics Research C, Vol. 26, 1–12, 2012

250 MHZ TO 30 GHZ, UNILATERAL CIRCUIT MODEL FOR INGAP/GAAS HBT

T. T. Thein*, **C. L. Law, and K. Fu**

Positioning and Wireless Technology Center, 50 Nanyang Drive, Research TechnoPlaza, Nanyang Technological University, 637553, Singapore

Abstract—A unilateral circuit model, which precisely predicts small signal response over a wide range of frequencies and bias points, is quantitatively analyzed and presented. The shortfall of current unilateral assumption and transformation technique is presented. A complete and explicit analysis is provided to develop a compact unilateral circuit model. The model is intended to predict input reflection, forward transmission and output reflection coefficients over wide range of frequencies. The technique is validated by transforming bilateral a small signal model of $3 \times 3\,\mu m \times 40\,\mu m$, InGaP/GaAs HBT into its unilateral equivalent over the frequency range of 250 MHz to 30 GHz. The accuracy of the technique is corroborated at various bias conditions; collector current from 3 mA to 150 mA and collector-emitter voltage from 1 V to 5 V. Simulated results show very good agreement between small signal responses of transformed unilateral and bilateral circuit models.

1. INTRODUCTION

Bilateral equivalent circuit models for the active device are extensively used for circuit simulation in various design processes. These design processes often uses optimization to achieve the design goals which often do not result in optimal designs. Meanwhile, analytical formulations like distortion analysis [1, 2], non-linearity analysis [3–5], distributed amplifier design [1, 6] and other applications [7, 8] are derived based on simplified unilateral model assumption for the active device. In the area of model parameter extractions, many techniques,

Received 17 October 2011, Accepted 30 November 2011, Scheduled 5 December 2011

* Corresponding author: Than Tun Thein (N060107@e.ntu.edu.sg).

[9–11], have been presented to accurately extract active device small signal model parameters using bilateral model. However, there is lack of published work on the extraction of an ultra wideband unilateral model and the model parameters. Some research works [3, 4, 12] who have used simplified unilateral model for their analyses assume that the base-collector feedback capacitance and emitter feedback resistance are very small and are simply neglected. When the voltage gain is much greater than one, feedback capacitance effectively shape input impedance. Another researcher [1] used Miller approximation to account for the feedback network effect.

As the frequency of the signal being processed by a circuit increases the capacitive feedback elements in the circuit eventually become important. In another scenario, as the collector current level increase, the emitter feedback resistance becomes more significant. Without developing proper unilateral model, assuming and using simplified unilateral circuit in the analyses will introduce errors. The equivalent circuit after decoupling base and collector, using Miller approximation is only useful for calculating forward transmission and input impedance of the circuit. This is not useful for calculating output impedance [13, 14]. For nonlinear and distortion analysis, input and output impedances at difference frequencies are crucial. Without output impedance information, performance characterization will not be completely valid. [15] developed a HBT unilateral model oriented to fast prediction of the performance of distributed amplifiers.

In this paper, we develop a unilateral model that can predict input impedance, gain and output impedance over a wide range of frequency and at different bias points. Transformation equations taking into account all extrinsic elements in the bilateral model into the unilateral model of a $3 \times 3\,\mu\text{m} \times 40\,\mu\text{m}$ InGaP/GaAs HBT to its unilateral equivalent over the frequency range of 250 MHz to 30 GHz. The accuracy of the technique is also validated at various bias points; collector current ranging from 3 mA to 150 mA and collector voltage ranging from 1 V to 5 V. Very good agreement is achieved between small signal responses of transformed unilateral model compare with the bilateral model.

2. SIMPLIFIED UNILATERAL AND MILLER APPROXIMATION PERFORMANCE

Figure 1 presents the bilateral small-signal equivalent circuit model of InGaP/GaAs HBTs. The model is based on the well-known hybrid-pi equivalent circuit, directly extracted from S-parameter data, without employing any optimization and using the technique presented in [9].

Fig. 1(b) shows the extracted parameters of each component for the bias point of $Ic = 39\,\text{mA}$ and $Vce = 4\,\text{V}$.

The bilateral model incorporates with two feedback networks, emitter resistance (r_{ee}) and base-collector junction capacitance (C_μ). The extracted emitter resistance is $0.2\,\Omega$, which is bias independent and is assumed to be negligible at low collector current levels. However, the voltage drop across it is about 20 mV when the collector current reaches

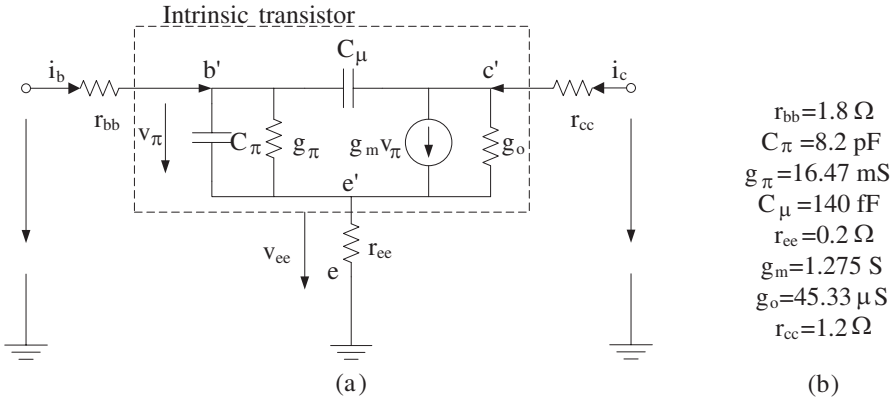

Figure 1. Bilateral small signal equivalent circuit model (a) and extracted circuit parameters (b).

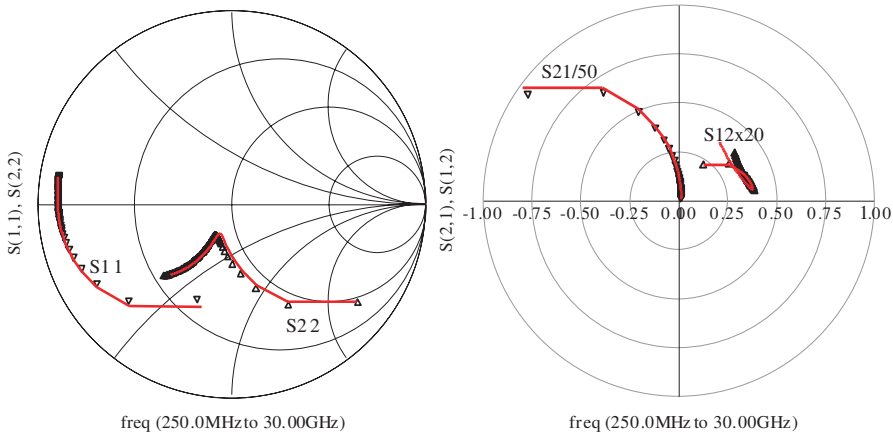

Figure 2. Measured S-parameter responses (symbol) and simulated bilateral model response (solid line).

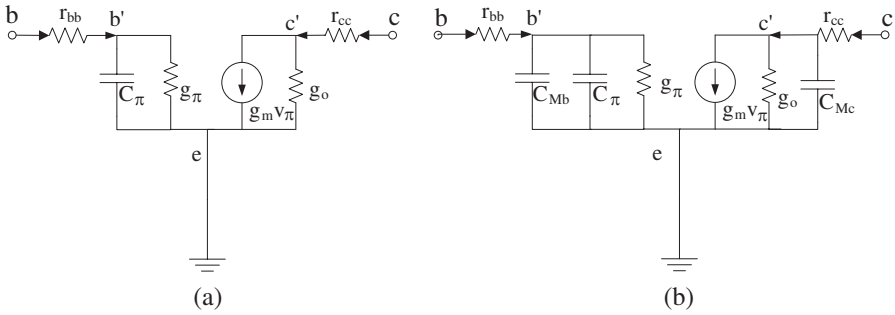

Figure 3. Simplified unilateral circuit model (a) and Miller approximated circuit model (b).

100 mA, which is 66% of maximum operating current. This amount of feedback voltage is large enough to offset the base bias point. To develop a more robust circuit model, we assume r_{ee} is a substantial feedback element. The extracted bias dependent, C_μ is 147 fF. The reactance of this feedback path changes from 4.33 kΩ at 250 MHz to 36 Ω at 30 GHz. This suggests baseband, fundamental and harmonics will experience difference impedances. Any assumption applied on this feedback element based on specific frequency for nonlinear analyses is incomplete.

Simplified unilateral and Miller approximated circuits are simulated and their validity are analyzed. 50 Ω load is assumed in Miller capacitance computation. The circuits used for simulation are shown in Fig. 3 and S-parameter responses of bilateral, simplified unilateral and Miller approximation, are shown in Fig. 4. Simplified unilateral circuit responses are significantly different from bilateral data for S_{11} and S_{21}, even at the frequency as low as 250 MHz. Mean while, as mention before, Miller approximation gives very close responses for S_{11} and S_{21}. However, both circuits completely fail to predict S_{22}. In addition, S_{22} is not following a constant conductance circle in the Smith chart and it is rather switches from constant resistance to constant conductance above the resonance frequency.

3. ANALYSIS FOR UNILATERAL CIRCUIT MODEL

3.1. Decoupling r_{ee}

A quantitative analysis is applied on bilateral circuit shown in Fig. 1. Emitter resistance is uncoupled in the first step. The small signal base and collector current of the intrinsic transistor located between b', c'

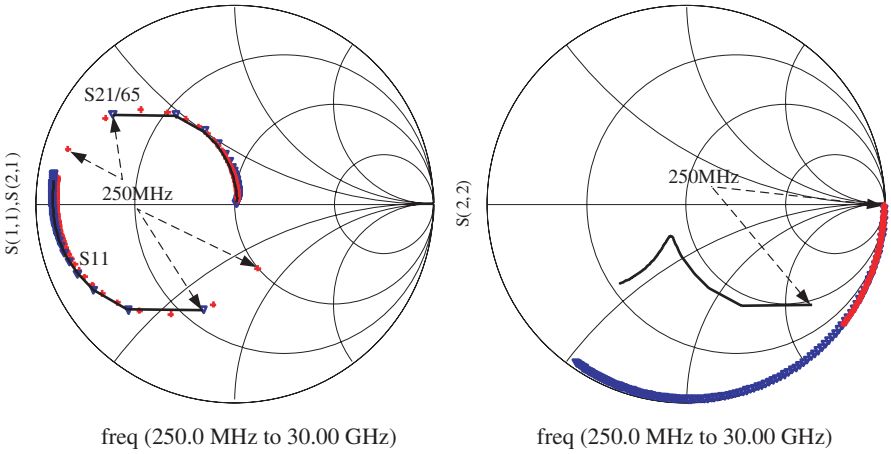

Figure 4. Simulated S-parameter responses of bilateral (black solid line), simplified unilateral (red cross) and Miller approximated (blue triangle) circuit models.

and e' can be presented as in [16],

$$i_b = (Y_{\pi 1} + j\omega C_\mu)\, v_{b'} - (g_{\mu 1} + j\omega C_\mu)\, v_{c'} \tag{1}$$

$$i_c = (g_{m1} - j\omega C_\mu)\, v_{b'} + (g_{o1} + j\omega C_\mu)\, v_{c'} \tag{2}$$

where,

$$\begin{aligned} Y_{\pi 1} &= Y_\pi \left[\frac{(1+r_{ee}g_o)}{1+r_{ee}(Y_\pi+g_m+g_o)}\right], g_{\mu 1} = g_o \left[\frac{r_{ee}Y_\pi}{1+r_{ee}(Y_\pi+g_m+g_o)}\right] \\ g_{m1} &= g_m \left[\frac{1-r_{ee}g_oY_\pi/g_m}{1+r_{ee}(Y_\pi+g_m+g_o)}\right], g_{o1} = g_o \left[\frac{1+r_{ee}Y_\pi}{1+r_{ee}(Y_\pi+g_m+g_o)}\right] \end{aligned} \tag{3}$$

where, $Y_\pi = g_\pi + j\omega C_\pi$. Generally, for HBT, g_o is very small (also in our case) and can be neglected. However, for the sake of model completeness for the transistor with larger g_o, it is included in the formulation. In the case where Y_π is much smaller than g_m (with g_o neglected), (3) will reduced to local series-series feedback concept shown in [13, 17, 18]. With some necessary circuit elements modification as in (3), emitter resistance is uncoupled. As long as g_o is concerned, an additional conductance is needed to add in parallel with C_μ. The effective base-emitter admittance ($Y_{\pi 1}$), transconductance (g_{m1}) and output conductance (g_{o1}) are smaller than original value. Mean while C_μ is unaffected. The resultant equivalent circuit after uncoupling r_{ee} is presented in Fig. 5.

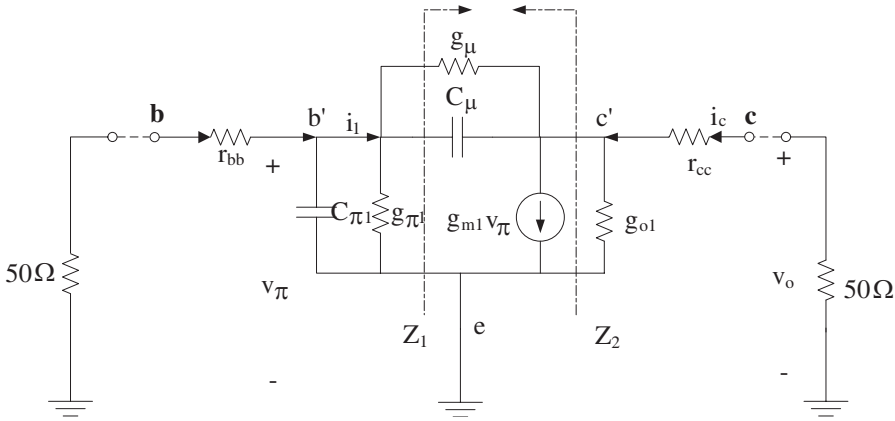

Figure 5. Equivalent circuit after r_{ee} uncoupled (intermediate state).

3.2. Decoupling Z_μ

Decoupling the feedback, $Z_\mu = (g_\mu + j\omega C_\mu)^{-1}$, between base and collector requires us to quantify equivalent impedances Z_1 (looking toward load) and Z_2 (looking toward source) as shown in Fig. 5. They are specified under the condition that the input and output port are terminated with $50\,\Omega$.

3.2.1. The Impedance Z_1

Analyzing current i_1, shown in Fig. 5, flowing into Z_μ gives Z_1 as,

$$Z_1 = \left[(g_\mu + j\omega C_\mu)\,(1 + g_{m1} Z_0) \left(\frac{1 - \dfrac{(g_\mu + j\omega C_\mu)}{g_{m1}}}{1 + g_o Z_l + Z_l\,(g_\mu + j\omega C_\mu)} \right) \right]^{-1} \tag{4}$$

where, $Z_l = Z_0 + r_{cc}$. As shown in (4), Z_1 is frequency dependent. However, neglecting g_μ and low frequency analysis will yield Z_1 to be the impedance of the Miller approximation equivalent.

3.2.2. The Impedance Z_2

Then equivalent output impedance, Z_2, can be express as,

$$Z_2 = \left[Z'_{\pi 1} + Z_\mu \right] \Big\| \left[\left(g_{m1} Z'_{\pi 1} \right) \Big/ \left(Z'_{\pi 1} + Z_\mu \right) \right] \tag{5}$$

where, $Z'_{\pi 1} = [(Z_0 + r_{bb}) \| Z_{\pi 1}]$, and the real and imaginary parts of Z_2 can be express as,

$$\begin{aligned} \mathrm{Re}Z_2 &= \frac{g_T A + \omega^2 C_T B}{A^2 + \omega^2 B^2}, \qquad \mathrm{Im}Z_2 = -j\omega \frac{g_T B - C_T A}{A^2 + \omega^2 B^2} \\ A &= \left[g_\mu \left(g'_{\pi 1} + g_{m1} \right) - \omega^2 C'_{\pi 1} C_\mu \right], \; B = \left[C_\mu \left(g'_{\pi 1} + g_{m1} \right) - C'_{\pi 1} g_\mu \right] \end{aligned} \tag{6}$$

where, $g_T = g'_{\pi 1} + g_\mu$ and $C_T = C'_{\pi 1} + C_\mu$. Equation (6) provides an inclusive close form formula for impedance Z_2 without pre-assumption and neglected circuit elements. However, for our transistor g_o is very small and so related terms are negligible. Then (6) can be simplified into,

$$\begin{aligned} \mathrm{Re}Z_2 &= \frac{-\omega^2 g'_{\pi 1} C'_{\pi 1} C_\mu + \omega^2 C_T \left(g'_{\pi 1} + g_{m1} \right)}{\left(\omega^2 C'_{\pi 1} C_\mu \right)^2 + \omega^2 C_\mu^2 \left(g'_{\pi 1} + g_{m1} \right)^2} \\ \mathrm{Im}Z_2 &= -j\omega \frac{\omega^2 C_T C'_{\pi 1} C_\mu + C_\mu g'_{\pi 1} \left(g'_{\pi 1} + g_{m1} \right)}{\left(\omega^2 C'_{\pi 1} C_\mu \right)^2 + \omega^2 C_\mu^2 \left(g'_{\pi 1} + g_{m1} \right)^2} \end{aligned} \tag{7}$$

Equation (7) is the same formula used in [17, 18] with no g_o consideration. This proofs the robustness of the formulation. As shown in Fig. 4, S_{22} is switching from series R-C at low frequencies to shunt R-C behavior at high frequencies. Hence, frequency limit is imposed and under low frequency analysis, Equation (7) can be further simplified into,

$$\begin{aligned} \mathrm{Re}Z_2 = R_2 &\approx \frac{C'_{\pi 1}}{C_\mu} \frac{g_{m1}}{(g'_{\pi 1} + g_{m1})^2} + \frac{1}{(g'_{\pi 1} + g_{m1})} \\ \mathrm{Im}Z_2 = \frac{1}{j\omega C_2} &\approx -j \frac{g'_{\pi 1}}{\omega C_\mu (g'_{\pi 1} + g_{m1})} \end{aligned} \tag{8}$$

Equation (8) shows at low frequencies Z_2 can be seen as a series network of a resistance (R_2) and a capacitance (C_2). This agrees with bilateral S_{22} response shown in Fig. 2. At high frequencies,

$$\begin{aligned} \mathrm{Re}Y_2 = \frac{1}{R_3} &\approx g'_{\pi 1} \left(\frac{C_\mu}{C_T} \right)^2 + \frac{g_m C_\mu}{C_T} \\ \mathrm{Im}Y_2 = j\omega C_3 &\approx j\omega \frac{C_\mu C_{\pi 1}}{C_T}, Y_2 = \frac{1}{Z_2} \end{aligned} \tag{9}$$

In (9), R_3 and C_3 are in parallel. Again, this also follows S_{22} response at high frequency.

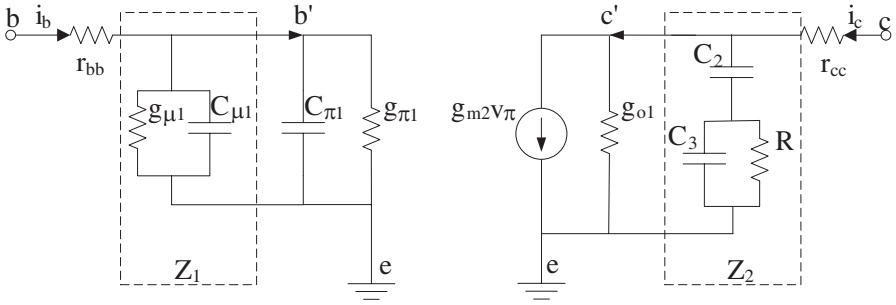

Figure 6. Modified complete unilateral circuit model.

3.2.3. The Transconductance g_m

As the output network is being modified, the transconductance (g_{m1}) is compensated as,

$$g_{m2} = g_{m1} \left| Z_m \right| e^{i\theta_m} \tag{10}$$

where, $Z_m = (Z_0 + Z_2)/Z_2$ and g_{m2} is strongly varying in the frequency region of < 5 GHz.

Equations (8) and (9) will yield two different R-C values. However, numerical valuation at different bias points revel that R_2 and R_3 have slightly different values (6% of their absolute values). Hence, we select a resistance (R), which is a mean of R_2 and R_3. Complete unilateral equivalent circuit model is presented in Fig. 6. Note that a single resistor is presented in Z_2 network for both low and high frequencies.

4. SIMULATED RESULTS AND DISCUSSION

In order to validate and evaluate the accuracy of the proposed technique, we transform the bilateral model shown in Fig. 1 into unilateral. Table 1 gives the computed unilateral model parameter values using the aforementioned technique. Both g_o and g_μ are neglected in the simulation. g_{m2} is defined as frequency dependent parameter. The circuit models are simulated in Agilent's Advance Design System. Parasitic contact inductances of $L_b = 20.17$ pH, $vL_c = 18.532$ pH and $L_e = 5$ pH are included in the simulation. Fig. 7 shows the comparison of S-parameters generated from the bilateral and unilateral model for the bias point of $Ic = 39$ mA and $Vcc = 4$ V. Very good agreements over the frequency range of 250 MHz to 30 GHz are obtained. The robustness of the technique is investigated at various bias points. Bilateral parameters, extracted for various

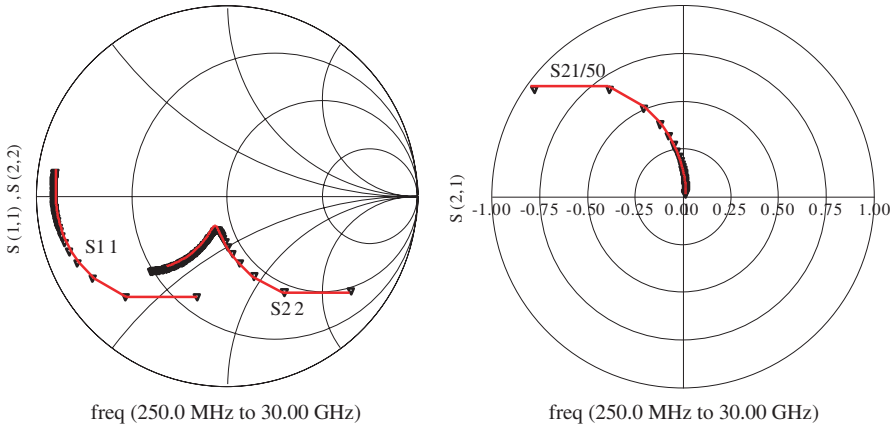

Figure 7. Simulated S-parameter response of bilateral (red lines) and developed unilateral (black triangle) circuit models for $Vcc = 4\,\mathrm{V}$ and from $Ic = 39\,\mathrm{mA}$.

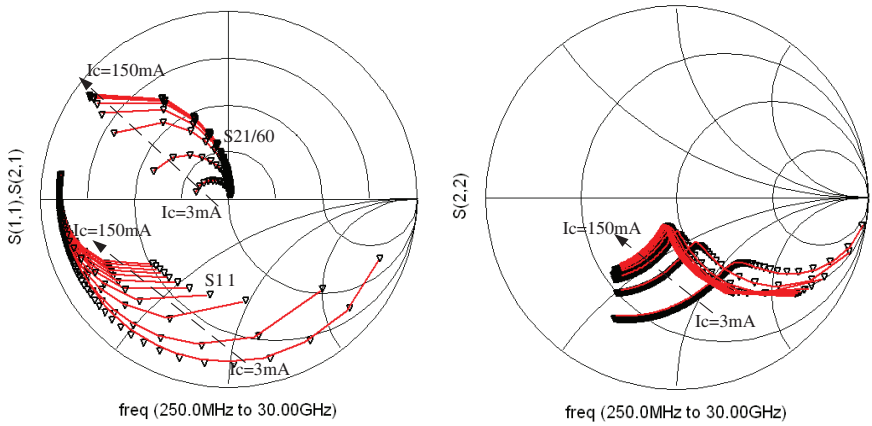

Figure 8. Simulated S-parameter response of bilateral (red lines) and developed unilateral (black triangle) circuit models for $Vcc = 5\,\mathrm{V}$ and from $Ic = 3\,\mathrm{mA}$ to $150\,\mathrm{mA}$.

collector currents ($3\,\mathrm{mA}$ to $150\,\mathrm{mA}$) at $V_{cc} = 5\,\mathrm{V}$, are used to develop unilateral equivalent circuit models. Fig. 8 shows the overlay plot of simulated unilateral and bilateral S-parameters data.

Unilateral responses agree very well with bilateral response for all collector currents. This indicates that the technique is robust and applicable for different bias sets. This modeling technique will be useful

Table 1. Computed unilateral parameters for $Ic = 39\,\text{mA}$ and $Vcc = 4\,\text{V}$.

$r_{bb} = 1.8\,\Omega$	$C_{\mu 1} = 8.02\,\text{pF}$	$C_{\pi 1} = 6.5\,\text{pF}$
$g_{\pi 1} = 113\,\text{mS}$	$g_{m1} = 1.016\,\text{S}$	$C_2 = 4.7\,\text{pF}$
$C_3 = 135\,\text{fF}$	$R = 43.5\,\Omega$	$r_{cc} = 1.2\,\Omega$

for RF circuit designers, who have limited resources to use or develop large signal full electro-thermal models such as VBIC and GP for pre-fabrication analysis, can develop relatively accurate small signal model over wide range of bias points and frequency, using a hand full of S-parameter measurements. The model also give detail understanding of small signal nonlinear mechanism and frequency dependent impedance behaviors of the device.

5. CONCLUSION

Quantitative analysis has been conducted to develop a unilateral circuit model for simulation and numerical analysis. Without pre-assumption all intrinsic and extrinsic elements (except parasitic) of the transistor are accounted in the formulation. Possible formula reduction base on specific assumption are also highlighted. A complete and explicit unilateral model is presented. The technique is validated through unilateral transformation of bilateral model extracted at $Ic = 39\,\text{mA}$ and $Vcc = 4\,\text{V}$, over the frequency range of 250 MHz to 30 GHz. All three bilateral S-parameter data are accurately predicted by unilateral model. The robustness of the transformation procedure is investigated with bilateral parameters extracted from different bias points. Simulated results confirmed that the agreement is achieved over wide range of collector current levels.

ACKNOWLEDGMENT

This work was supported by the ASTAR project under the Grant 062-101-0029. The authors would like to acknowledge the support of the ASTAR.

REFERENCES

1. Van Der Heijden, M., et al., "On the optimum biasing and input out-of-band terminations of linear and power efficient class-

AB bipolar RF amplifiers," *IEEE Proceedings of the Meeting on Bipolar/BiCMOS Circuits and Technology*, 2004.

2. El Maazouzi, L., A. Mediavilla, and P. Colantonio, "A contribution to linearity improvement of a highly efficient PA for WIMAX applications," *Progress In Electromagnetics Research*, Vol. 119, 59–84, 2011.
3. Iwamoto, M., et al., "Optimum bias conditions for linear broadband InGaP/GaAs HBT power amplifiers," *IEEE Trans. Micro. Theory Tech.*, Vol. 50, No. 12, 2954–2962, 2002.
4. Van Der Heijden, M. P., et al., "Theory and design of an ultralinear square-law approximated LDMOS power amplifier in class-AB operation," *IEEE Trans. Micro. Theory Tech.*, Vol. 50, No. 9, 2176–2184, 2002.
5. Karkhaneh, H., A. Ghorbani, and H. Amindavar, "Modeling and compensating memory effect in high power amplifier for OFDM system," *Progress In Electromagnetics Research*, Vol. 3, 183–194, 2008.
6. Olson, S., B. Thompson, and B. Stengel, "Distributed amplifier with narrowband amplifier efficiency," *IEEE International Microwave Simposium*, 155–158, Honolulu, USA, 2007.
7. Sheinman, B. and C. Ritter, "Base charge dynamics of abrupt base-emitter junction HBTs and its representation in transistor models," *IEEE Trans. Electron Devices*, Vol. 54, No. 4, 632–636, 2007.
8. Zhao, Y., et al., "Linearity improvement of HBT-based Doherty power amplifiers based on a simple analytical model," *IEEE Trans. Micro. Theory Tech.*, Vol. 54, No. 12, 4479–4488, 2006.
9. Lee, K., et al., "Direct parameter extraction of SiGe HBTs for the VBIC bipolar compact model," *IEEE Trans. Electron Devices*, Vol. 52, No. 3, 375–384, 2005.
10. Yang, T. R., et al., "SiGe HBT's small-signal Pi modeling," *IEEE Trans. Micro. Theory Tech.*, Vol. 55, No. 7, 1417–1424, 2007.
11. Olvera-Cervantes, J. L., et al., "A new analytical method for robust extraction of the small-signal equivalent circuit for SiGe HBTs operating at cryogenic temperatures," *IEEE Trans. Micro. Theory Tech.*, Vol. 56, No. 3, 568–574, 2008.
12. Spirito, M., et al, "Experimental procedure to optimize out-of-band terminations for highly linear and power efficient bipolar class-AB RF amplifiers," *IEEE Proceedings of the Meeting on Bipolar/BiCMOS Circuits and Technology*, 112–115, 2005.

13. Gray, P. R., et al., *Analysis and Design of Analog Integrated Circuits*, Wiley, New York, USA, 1993.
14. Everard, J., J. Wiley, and I. Sons, *Fundamentals of RF Circuit Design*, Wiley Online Library, 2001.
15. Paoloni, C. and S. D'Agostino, "An HBT unilateral model to design distributed amplifiers," *IEEE Trans. Micro. Theory Tech.*, Vol. 47, No. 6, 795–798, 1999.
16. Reisch, M., *High-frequency Bipolar Transistors: Physics, Modelling, Applications*, Springer Verlag, 2003.
17. Tu, H. Y., et al., "An analysis of the anomalous dip in scattering parameter S_{22} of InGaP-GaAs heterojunction bipolar transistors (HBTs)," *IEEE Trans. Electron Devices*, Vol. 49, No. 10, 1831–1833, 2002.
18. Lu, S. S., et al., "The origin of the kink phenomenon of transistor scattering parameter S_{22}," *IEEE Trans. Micro. Theory Tech.*, Vol. 49, No. 2, 333–340, 2001.